

## Thermal Analysis of Organic Light Emitting Diodes Based on Basic Heat Transfer Theory

This content has been downloaded from IOPscience. Please scroll down to see the full text.

2015 Chinese Phys. Lett. 32 087201

(<http://iopscience.iop.org/0256-307X/32/8/087201>)

View [the table of contents for this issue](#), or go to the [journal homepage](#) for more

Download details:

IP Address: 202.117.17.90

This content was downloaded on 18/12/2016 at 11:35

Please note that [terms and conditions apply](#).

You may also be interested in:

[Emiflective Display with Integration of Reflective Liquid Crystal Display and Organic Light Emitting Diode](#)

Bo-Ru Yang, Kang-Hung Liu and Han-Ping D. Shieh

[Enhancement of Barrier Properties Using Ultrathin Hybrid Passivation Layer for Organic Light Emitting Diodes](#)

Sung Jin Bae, Joo Won Lee, Jung Soo Park et al.

[New Fraction Time Annealing Method For Improving Organic Light Emitting Diode Current Stability of Hydrogenated Amorphous Silicon Thin-Film Transistor Based Active Matrix Organic Light Emitting Diode Backplane](#)

Jae-Hoon Lee, Sang-Geun Park, Jae-Hong Jeon et al.

[Thermal analysis of IRT-T reactor fuel elements](#)

A Naymushin, Yu Chertkov, I Lebedev et al.

[Active Matrix Organic light Emitting Diode Display Based on "Super Top Emission" Technology](#)

Tadashi Ishibashi, Jiro Yamada, Takashi Hirano et al.

[Thermal analysis of superconducting undulator cryomodules](#)

Y Shiroyanagi, C Doose, J Fuerst et al.

[Thermal analysis and microstructural characterization of Mg-Al-Zn system alloys](#)

M Król, T Taski and W Sitek

[Thermal analysis of the mixtures of paraffin with aluminum in wide temperature range](#)

S A Gubin, I V Maklashova and I S Levitskaya

## Thermal Analysis of Organic Light Emitting Diodes Based on Basic Heat Transfer Theory \*

ZHANG Wen-Wen(张稳稳)<sup>1\*\*</sup>, WU Zhao-Xin(吴朝新)<sup>2</sup>, LIU Ying-Wen(刘迎文)<sup>3</sup>, DONG Jun(董军)<sup>1</sup>,  
YAN Xue-Wen(严学文)<sup>1</sup>, HOU Xun(侯洵)<sup>2</sup>

<sup>1</sup>School of Electronic Engineering, Xi'an University of Post & Telecommunication, Xi'an 710121

<sup>2</sup>Key Laboratory for Physical Electronics and Devices of the Ministry of Education, & Key Laboratory of Photonics Technology for Information of Shaanxi Province, School of Electronic and Information Engineering, Xi'an Jiaotong University, Xi'an 710049

<sup>3</sup>MOE Key Laboratory of Thermo-Fluid Science and Engineering, School of Energy and Power Engineering, Xi'an Jiaotong University, Xi'an 710049

(Received 11 February 2015)

We investigate the thermal characteristics of standard organic light-emitting diodes (OLEDs) using a simple and clear 1D thermal model based on the basic heat transfer theory. The thermal model can accurately estimate the device temperature, which is linearly with electrical input power. The simulation results show that there is almost no temperature gradient within the OLED device working under steady state conditions. Furthermore, thermal analysis simulation results show that the surface properties (convective heat transfer coefficient and surface emissivity) of the substrate or cathode can significantly affect the temperature distribution of the OLED.

PACS: 72.80.Le, 85.60.Jb, 68.60.Dv

DOI: 10.1088/0256-307X/32/8/087201

Organic light-emitting diodes (OLEDs), which were first reported by Tang *et al.*<sup>[1]</sup> in 1980s, have received considerable attention due to their potential applications in flat panel displays and lighting. A particular challenge in achieving intense OLED sources for illumination or other applications is to remove heat efficiently.<sup>[2]</sup> This is due to the fact that the joule heat can accelerate degradation of the organic active materials under the high currents required, such as reducing brightness homogeneity, and reducing luminance, short lifetime, large spectral shift.<sup>[3–7]</sup> Thermal analysis and improvement in the thermal stability of OLEDs are essential for progress in their practical applications, especially for large area devices where joule heating can be substantial.<sup>[8,9]</sup> Therefore, many research groups devoted to discuss thermal characteristics of the OLEDs.<sup>[4–11]</sup>

It is important to quantitatively understand the thermal environment of the multilayer composite device under high current operation, and then to mitigate the effects of heating by optimization design of devices and systems.<sup>[2]</sup> Thus a simple and clear thermal model of OLEDs for thermal analysis plays an important role as mentioned above. Some models have been proposed. For example, Qi *et al.* completed thermal analysis of high intensity organic light-emitting diodes based on a transmission matrix approach.<sup>[2]</sup> Park *et al.* implemented a comprehensive 1D numerical model in which Poisson's equation, drift-diffusion equation, and heat flow equation are coupled

to one another.<sup>[12]</sup> However, few OLED thermal analysis models involve the basic heat transfer theory. As we know, there are three modes of heat transfer: conduction, convection and radiation. It is easy to understand and more intuitive relative to deep technical semiconductor physics and semiconductor devices. In this work, we calculate the thermal properties of OLEDs using a simple and clear 1D thermal model based on the basic heat transfer theory.

Verified by experimental data in the literature,<sup>[13]</sup> the thermal model can accurately estimate the device temperature. The calculated results show that there is almost no temperature gradient inside the OLED device working under steady state conditions. Also, the simulated results show that the device temperature can be reduced by some ways, e.g., the surface emissivity is increased by improving surface properties, or the convective heat transfer coefficient is increased by forced convection. In short, this model can be used to study the thermal analysis of an OLED.

This work focuses on a standard OLED (Fig. 1) and implements a comprehensive 1D thermal model base on the basic heat transfer theory. The operating OLED device should satisfy the following relations: the input electric power is equal to the sum of the increased internal energy of the device, light energy consumption, as well as heat dissipation through convection and radiation to ambient environment.

A typical OLED device consists of multilayer films with hundreds of nanometers or less thickness and the

\*Supported by the National Natural Science Foundation of China under Grant No 11304247, the Shaanxi Provincial Research Plan for Young Scientific and Technological New Stars (No 2015KJXX-40), and the Youth Foundation of Xi'an University of Post & Telecommunication under Grant Nos 1011215 and 1010473.

\*\*Corresponding author. Email: zhangwenwen@xupt.edu.cn

© 2015 Chinese Physical Society and IOP Publishing Ltd

area of device is about dozens of  $\text{mm}^2$ . The thickness of the OLED device is four orders of magnitude smaller than the side length of its respective layer. Therefore, the heat transfer problems of the OLED devices can be as a one-dimensional plane wall heat transfer problem in large-area multilayer films. Some assumptions and simplifications are required to ensure that a model is not unwieldy and to allow mathematical solution.

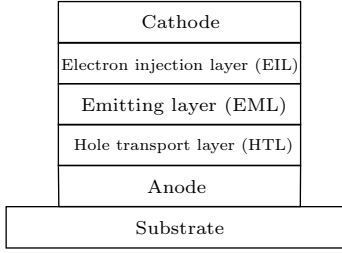


**Fig. 1.** Schematic view of the bilayer OLED structure.

(i) In the OLED element, holes and electrons injected from the anode and cathode, respectively, are recombined in the light emissive layer to excite organic molecules forming the light and non-radiative recombine to generate heat. It is well known that the induced high carrier concentration along with the electric field generate severe heat in the organic films.<sup>[12,14]</sup> In general, the recombination zone of carrier is near HTL/EML interface or in the EML,<sup>[12,15,16]</sup> and a high electric field is induced near the interface inside the electron transport layer (ETL) layer.<sup>[12,17,18]</sup> A standard OLED as shown in Fig. 1, the material of EML is used as both EML and ETL. Thus we assume that the EML is a uniform inner heat source.

(ii) The thermal model of the OLED is considered as the constant material model. Due to the fact that the thickness of the OLED device is very small, and the variation of temperature changes in the thickness direction is less than  $10^\circ\text{C}$ , the material physical properties in the thickness direction is ignored.

(iii) For simplicity, the contact resistance between the OLED functional layers is not considered in the current calculation.

We establish the thermal resistance model of the total OLED device, as shown in Fig. 2. The upper and lower surface temperatures of the EML layer are recorded as  $T_{\text{EMLup}}$  and  $T_{\text{EMLdown}}$ , respectively. The upper and lower surface temperatures of the glass substrate are recorded as  $T_{\text{gup}}$  and  $T_{\text{gdown}}$ , respectively. The surface temperature of cathode is recorded as  $T_{\text{cathode}}$ . The ambient temperature is recorded as  $T_{\text{sur}}$ . In Fig. 2, thermal resistance analysis is started from the interface temperature  $T_{\text{EMLup}}$  and  $T_{\text{EMLdown}}$ . This is due to the fact that the EML layer has an inner heat source. The thermal resistance analysis can not be applied for quantitative analysis due to the fact that the

heat flow is different for each  $x$ -section. Conductive thermal resistance, convective thermal resistance and radiative thermal resistance are recorded as  $D_{\text{res}}$ ,  $V_{\text{res}}$  and  $R_{\text{res}}$ , respectively.

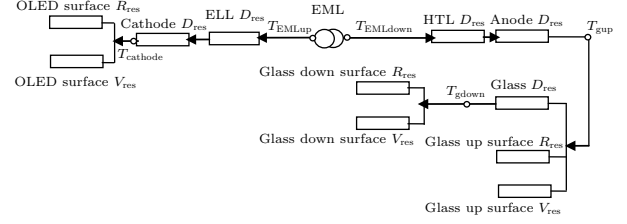


**Fig. 2.** The thermal resistance analysis model for the OLED device.

According to the law of conservation of energy,  $\Phi_1$  is equal to the total heat exchange of the glass substrate, the anode layer and a hole transport layer,  $\Phi_2$  is equal to the total heat exchange of the electron injection layer and the cathode layer, and  $\Phi$  is the total heat generated from the light-emitting layer. The majority of the energy of the injected charges results in Joule heating rather than light emission for the OLED device.<sup>[3]</sup> Thus it is assumed that all the electrical input is converted to heat. From Fig. 2, the following relations is satisfied,

$$\phi = \phi_1 + \phi_2 = P, \quad (1)$$

$$\phi_1 = \frac{T_{\text{EMLup}} - T_{\text{cathode}}}{\delta_{\text{Cathode}}/(\lambda_{\text{Cathode}}A_{\text{Cathode}}) + \delta_{\text{EIL}}/(\lambda_{\text{EIL}}A_{\text{EIL}})}, \quad (2)$$

$$\phi_1 = h(T_{\text{Cathode}} - T_{\text{sur}})A_{\text{Cathode}} + \varepsilon_{\text{Cathode}}\sigma[T_{\text{Cathode}}^4 - T_{\text{sur}}^4]A_{\text{Cathode}}, \quad (3)$$

$$\phi_2 = \frac{T_{\text{EMLdown}} - T_{\text{gup}}}{\delta_{\text{Anode}}/(\lambda_{\text{Anode}}A_{\text{Anode}}) + \delta_{\text{HTL}}/(\lambda_{\text{HTL}}A_{\text{HTL}})}, \quad (4)$$

$$\phi_2 = h(T_{\text{gup}} - T_{\text{sur}})(A_{\text{g}} - A_{\text{Cathode}}) + \varepsilon_{\text{g}}\sigma(T_{\text{gup}}^4 - T_{\text{gdown}}^4)(A_{\text{g}} - A_{\text{Cathode}}) + \frac{T_{\text{gup}} - T_{\text{gdown}}}{\delta_{\text{g}}/\lambda_{\text{g}}}A_{\text{g}}, \quad (5)$$

$$\frac{(T_{\text{gup}} - T_{\text{gdown}})}{\delta_{\text{g}}/\lambda_{\text{g}}}A_{\text{g}} = h(T_{\text{gdown}} - T_{\text{sur}})A_{\text{g}} + \varepsilon_{\text{g}}\sigma[T_{\text{gdown}}^4 - T_{\text{sur}}^4]A_{\text{g}}, \quad (6)$$

where  $T$ ,  $\delta$ ,  $\lambda$ ,  $A$ ,  $\varepsilon$ ,  $h$ ,  $P$  and  $\sigma$  are the temperature, thickness, thermal conductivity, area, surface emissivity, convection heat transfer coefficient, input power and the Stefan-Boltzmann constant, respectively.

As described in the previous section, the EML is assumed as a uniform inner heat source model. A coordinate system is established. Set the HTL/EML interface as coordinate origin, the thickness direction of EML as the  $x$  axis with positive direction to the cathode. The temperature distributions of the EML are described by Poisson equation, as follows:

$$\frac{\partial^2 T(x)}{\partial x^2} + \frac{P}{\lambda_{\text{EML}}\delta_{\text{EML}}A_{\text{OLED}}} = 0, \quad (7)$$

where  $T(x)$  is the temperature of the EML film at point  $x$ ,  $\lambda_{\text{EML}}$  is the thermal conductivity of the EML film,  $\delta_{\text{EML}}$  is the thickness of the EML film, and  $A_{\text{OLED}}$  is the active emitting area. There are two boundary conditions:  $T(0) = T_{\text{EMLdown}}$  and  $T(\delta_{\text{EML}}) = T_{\text{EMLup}}$ .

Combination of the two boundary conditions,  $T(x)$ , as

$$T(x) = \frac{UI}{2\lambda_{\text{EML}}\delta_{\text{EML}}A_{\text{OLED}}}(\delta_{\text{EML}}x - x^2) + \frac{T_{\text{EMLup}} - T_{\text{EMLdown}}}{\delta_{\text{EML}}}x + T_{\text{EMLdown}}. \quad (8)$$

We already know that  $\Phi_1$  and  $\Phi_2$  are the heat flows at point 0 and at point  $\delta_{\text{EML}}$ , respectively. Thus

$$\frac{T_{\text{EMLup}} - T_{\text{EMLdown}}}{\delta_{\text{EML}}} + \frac{\phi_2}{\lambda_{\text{EML}}A_{\text{OLED}}} = \frac{P}{2\lambda_{\text{EML}}A_{\text{OLED}}}. \quad (9)$$

We can calculate the values of  $\Phi_1$ ,  $\Phi_2$ ,  $T_{\text{cathode}}$ ,  $T_{\text{gup}}$ ,  $T_{\text{gdown}}$ ,  $T_{\text{EMLup}}$  and  $T_{\text{EMLdown}}$  by simultaneous solution of Eqs. (1)–(9). Based on these parameters mentioned above, we can determine the temperature distribution and performed a thermal analysis of the OLED device.

We used a device structure of Ref. [13] to test the model. The devices structure consists of a 150-nm-thick indium-tin-oxide (ITO) pre-coated on a glass substrate, 60-nm-thick of poly(3, 4-ethylenedioxythiophene):poly(styrene sulfonate) (PEDOT:PSS) for an HTL, 60-nm-thick poly(9, 9-dioctylfluorene) (PFO) for an EML, 1.5-nm-thick lithium fluoride (LiF) for an EIL, and 150-nm-thick aluminum (Al) for cathode. Its schematic diagram [13] is shown in Fig. 3. The parameter values required for simulations are listed in Table 1. The ambient temperature is 35°C. [13] The thermal conductivity of POF is assumed to be the same as that of PEDOT:PSS. The thickness of glass substrate is assumed to be 1.2 mm. As shown in Fig. 4, our thermal model simulation results agreed well with the measured results in the literature. [13] However, we also see that our simula-

tion results are smaller than that of the literature under the high power density. It is well known that the luminance decreases while the input power increases during an OLED device running. It was not included in our simulation calculation that the increased input power is significant under the high power density, as might be responsible for smaller simulation results. In addition, the measured temperature was about 80°C under  $900 \text{ kW}\cdot\text{cm}^{-2}$ , which is close to softening temperature ( $T_s$ ) of the PFO. The polymers show morphological changes in the  $T_s$  region and the material physical properties might change, which might be the second factor for smaller simulation results. For all, the thermal model can accurately simulate the temperature of the device. Thus this model can be used to study the temperature distribution and its impact factors.

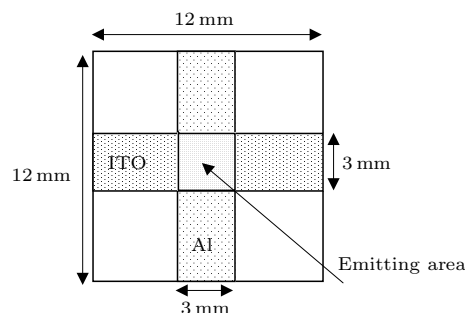


Fig. 3. The schematic diagram of the device in the literature.

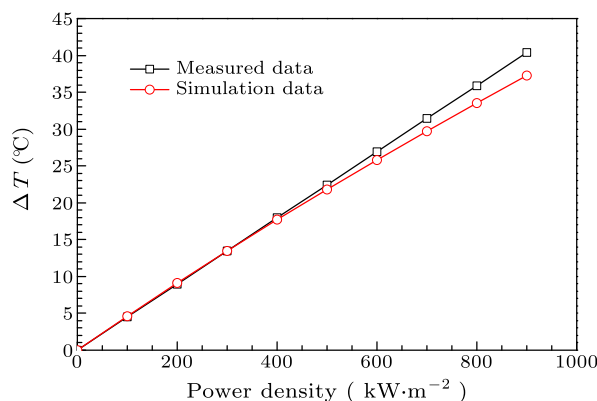


Fig. 4. The relationship between  $\Delta T$  and the power density of glass device.

Table 1. The parameter values required for simulations.

Parameter	Value
Glass surface emissivity ( $\epsilon_g$ )	0.8 <sup>[19]</sup>
Al surface emissivity ( $\epsilon_{\text{Cathode}}$ )	0.05 <sup>[20]</sup>
Convection heat transfer coefficient ( $h$ )	$2 \text{ W}\cdot\text{m}^{-2}\cdot\text{K}^{-1}$
Thermal conductivity of glass substrate ( $\lambda_g$ )	$1.05 \text{ W}\cdot\text{m}^{-1}\cdot\text{K}^{-1}$ <sup>[12]</sup>
Thermal conductivity of ITO ( $\lambda_{\text{Anode}}$ )	$12 \text{ W}\cdot\text{m}^{-1}\cdot\text{K}^{-1}$ <sup>[12]</sup>
Thermal conductivity of PEDOT:PSS ( $\lambda_{\text{HTL}}$ )	$0.17 \text{ W}\cdot\text{m}^{-1}\cdot\text{K}^{-1}$ <sup>[21]</sup>
Thermal conductivity of PFO ( $\lambda_{\text{EML}}$ )	$0.17 \text{ W}\cdot\text{m}^{-1}\cdot\text{K}^{-1}$
Thermal conductivity of LiF ( $\lambda_{\text{EIL}}$ )	$4.01 \text{ W}\cdot\text{m}^{-1}\cdot\text{K}^{-1}$ <sup>[22]</sup>
Thermal conductivity of Al ( $\lambda_{\text{Cathode}}$ )	$237 \text{ W}\cdot\text{m}^{-1}\cdot\text{K}^{-1}$ <sup>[13]</sup>

Figure 5 shows the temperature distribution of the device under  $900 \text{ kW}\cdot\text{cm}^{-2}$ . It can be seen that the temperature gradient inside the OLED is quite small when the OLED working under steady state conditions. This is consistent with the previous research.<sup>[12]</sup>

Figure 6 shows the device temperature with different convective heat transfer coefficients of the substrates. It can be seen that the device temperature can be greatly reduced when increasing the substrate convective heat transfer coefficient, especially in switching from natural to forced convection. When the convective heat transfer coefficient is increased to  $100 \text{ W}\cdot\text{m}^{-2}\cdot\text{K}^{-1}$ , the increase of device temperature slows down significantly. When the convective heat transfer coefficient of the substrate is smaller, the heat dissipation from OLED anode increases rapidly with increasing the substrate convective heat transfer coefficient. Thus the device temperature of the OLED sharply declines. However, when the convective heat transfer coefficient of the substrate increases to a certain limit, the heat dissipations from anode are close to the heat generated by the OLED. At this time, the temperature of the surface of the substrate is almost equal to the environmental temperature. From Fig. 7, we can see that the device temperature can be greatly reduced when increasing the substrate surface emissivity with similar reason.

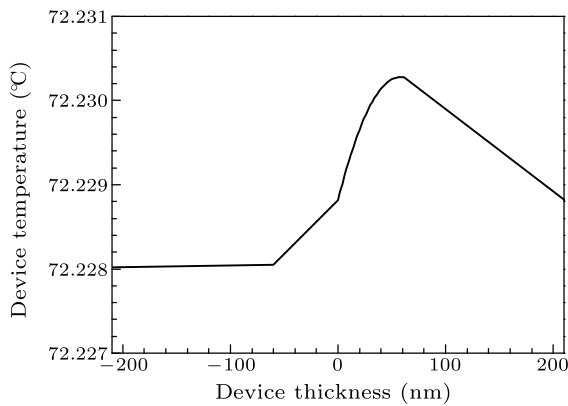


Fig. 5. Simulation results of temperature distributions inside the bilayer OLED.

Figure 8 shows the device temperature with different convective heat transfer coefficients of the cathode. It is shown that the device temperature reduced greatly when increasing the cathode convective heat transfer coefficient the same as increasing the substrate convective heat transfer coefficient. From Fig. 9, we can see that the device temperature is decreased almost linearly when increasing the cathode surface emissivity. This is due to the fact that the heat dissipation of the cathode surface is improved with increasing the cathode surface emissivity. However, the surface area of the cathode is much less than that of the substrate. The heat dissipation through the cathode surface is much smaller than that through the

substrate surface.

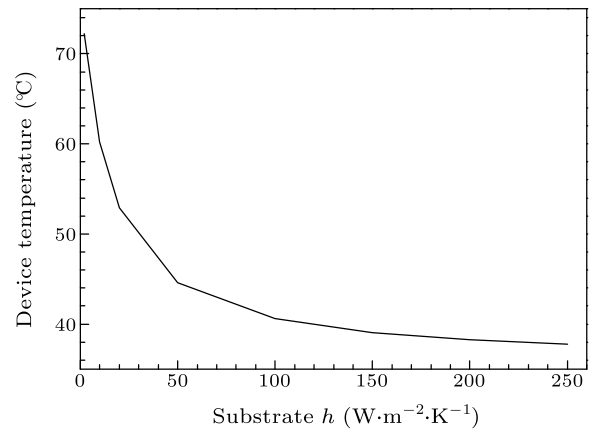


Fig. 6. Device temperatures versus convective heat transfer coefficient  $h$  of the substrate.

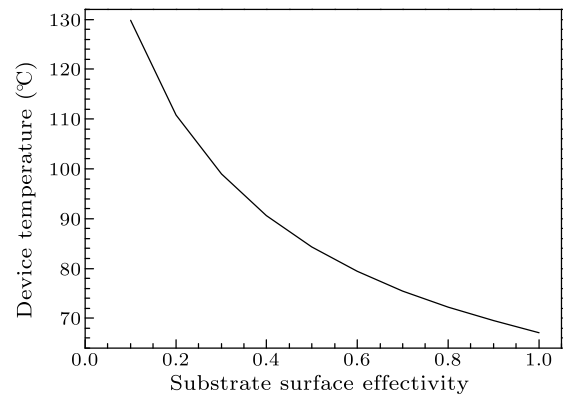


Fig. 7. Device temperatures with different substrate surface emissivities.

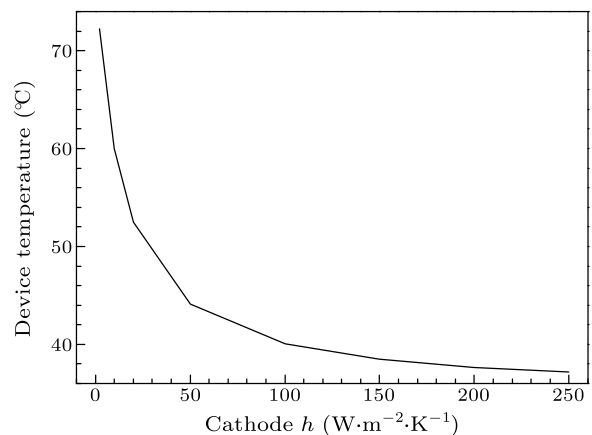
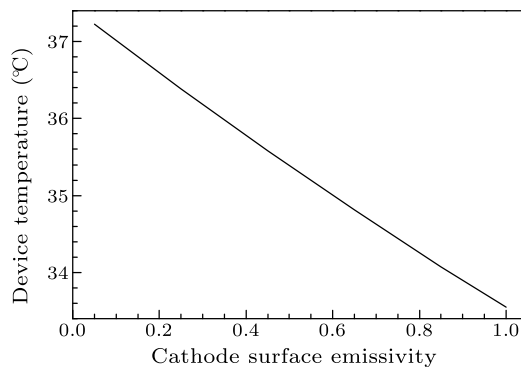


Fig. 8. Device temperatures with different cathode convective heat transfer coefficients ( $h$ ).

From what has been discussed above, the device temperature can reduce when increasing the surface emissivity and convective heat transfer coefficient of substrate or cathode. The above simulation is device temperature without encapsulation. In practice, the OLED was encapsulated to avoid oxygen and moisture. As shown in Fig. 1, glass was used as a substrate

for a bottom-emission OLED. The surface emissivity of the glass substrate is 0.8, much larger than that of the metal cathode, thus a practical approach of heat dissipation is adapted cathode encapsulation and heat sink, which has a higher surface emissivity.<sup>[12]</sup> The more effective approach to remove heat is by increasing convective heat transfer coefficient, such as increasing airflow velocity by fans, thermoelectric cooler.



**Fig. 9.** Device temperatures with different cathode surface emissivities.

In summary, a simple and clear 1D OLED thermal model based on the basic heat transfer theory has been implemented, and its feasibility has been verified by comparing with previous work. The temperature distribution of the function layer and substrate can be simulated according to this model. For a standard OLED working under steady state conditions, there is almost no temperature gradient within the organic films. For a given OLED, the device temperature can be accurately estimated by the thermal model in this study. Based on this model, the device temperature can be reduced with suitable ways, such as the surface emissivity is increased by improving surface properties, or the convective heat transfer coefficient is increased by forced convection. As a result, the model

can be applied to understand and control the temperature response of a range of important optoelectronic devices.

## References

- [1] Tang C W and VanSlyke S A 1987 *Appl. Phys. Lett.* **51** 913
- [2] Qi X and Forrest S R 2011 *J. Appl. Phys.* **110** 124516
- [3] Zhang W, Wu Z, Liang S, Jiao B, Zhang X, Wang D, Hou X, Chen Z and Gong Q 2011 *J. Phys. D: Appl. Phys.* **44** 155103
- [4] Boroumand F A, Voigt M, Lidzey D G, Hammiche A and Hill G 2004 *Appl. Phys. Lett.* **84** 4890
- [5] Garditz C, Winnacker A, Schindler F and Paetzold R 2007 *Appl. Phys. Lett.* **90** 103506
- [6] Zhou X, He J, Liao L S, Lu M, Ding X M, Hou X Y, Xiao Zhang M, He X Q and Lee S T 2000 *Adv. Mater.* **12** 265
- [7] Tessler N, Harrison N T, Thomas D S and Friend R H 1998 *Appl. Phys. Lett.* **73** 732
- [8] Sturm J C, Wilson W and Iodice H 1998 *IEEE J. Sel. Top. Quantum Electron.* **4** 75
- [9] Park J W, Shin D C and Park S H 2011 *Semicond. Sci. Technol.* **26** 034002
- [10] Bergemann K J, Krasny R and Forrest S R 2012 *Org. Electron.* **13** 1565
- [11] Kwak K, Cho K and Kim S 2013 *Opt. Express* **21** 29558
- [12] Park J, Ham H and Park C 2011 *Org. Electron.* **12** 227
- [13] Choi S H, Lee T I I, Baik H K, Roh H H, Kwon O and Sun D 2008 *Appl. Phys. Lett.* **93** 183301
- [14] Zhu J, Liu M, Wu B and Hou X Y 2012 *Chin. Phys. Lett.* **29** 097802
- [15] Bai J J, Wu X M, Hua Y L, Mu X, Bi W T, Su Y J et al 2013 *Chin. Phys. B* **22** 047806
- [16] Mu X, Wu X M, Hua Y L, Jiao Z Q et al 2013 *Chin. Phys. B* **22** 027805
- [17] Lee J H, Wu M H, Chao C C, Chen H L and Leung M K 2005 *Chem. Phys. Lett.* **416** 234
- [18] Book K, Nikitenko V R, B ässler H and Elschner A 2001 *J. Appl. Phys.* **89** 2690
- [19] Sagar D M, Aoudjane S, Gaudet M, Aeppli G and Dalby P A 2013 *Sci. Rep.* **3** 2130
- [20] Ridouane E H, Hasnaoui M and Campo A 2006 *Heat Mass Transfer R* **42** 214
- [21] Liu S, Hua D, Zhao Y et al 2015 *RSC. Adv.* **5** 1910
- [22] Zhao Y Q, Huang C J, Ogundimu T et al 2007 *Appl. Phys. Lett.* **91** 103109